Journal of High Energy Physics, Gravitation and Cosmology, 2025, 11(3), 850-868
https://www.scirp.org/journal/jhepgc
ISSN Online: 2380-4335
ISSN Print: 2380-4327

A Quantum Entangled Fractal Superfluid Universe

Otto Ziep

Independent Scholar, Berlin, Germany
Email: ottoziep@gmail.com

How to cite this paper: Ziep, O. (2025) A Quantum Entangled Fractal Superfluid Universe. *Journal of High Energy Physics, Gravitation and Cosmology*, **11**, 850-868.
https://doi.org/10.4236/jhepgc.2025.113054

Received: March 30, 2025
Accepted: July 8, 2025
Published: July 11, 2025

Abstract

The cosmological redshift, the expansion of the universe, the origin of cosmic rays including the microwave background is set in context to a fractal superfluid universe. Quantum entanglement is explained by highly correlated k-components of quadratic maps of curvature which captures growth of organic matter as well conductivity plateaus in layer structures. A mechanism of controlled ultra-high energy emission is discussed. A fractal superfluid universe model is capable to solve the cosmological constant problem, the Dirac monopole problem and the phenomenon of quantum entanglement for unified forces.

Keywords

Cosmic Rays, Cosmic Microwave Background, Apparent Universe Expansion, Cosmological Redshift, Conductivity Plateau, Air Ionization

1. Introduction

Gravitational field equations allow to regard stress-energy $T_{\mu\nu}$ as an equilibrium fluid or superfluid state [1]. From the viewpoint of coupling constants unified dimensionless fields as non-equilibrium, dimensionless states are capable to cover energy ranges of $10^2 \ldots 10^3$ orders of magnitude [2]. In macrophysics a pseudo-congruence on energy scale above 10^{20} eV as a fractal resolved potential difference explains the phenomenon of quantum entanglement (QE) for unified fields [3]. A fractal unified field allows to shift the origin of cosmic rays (CR) to a local bifurcating spacetime which explains also redshift and expansion of the universe by the influence of simplest cycles to vacuum susceptibilities. Experiments concerning the cosmological constant problem (CCP), QE and the Dirac monopole (DM) seem to prevent a unified theory of all forces [4]-[6]. The origin of CR is an open problem which is shifted to galactic forces. The present paper explains e.g. air ionization measured in vegetation areas by a bifurcating spacetime as a persistent non-equilibrium fractal zeta universe (FZU) [2]. Action $\mathcal{L}$ as Equation (14) is minimized for simplest cycles of chaotic quadruples of shifts $q_{sc} = \{1, \delta_k, \delta_k\delta_k, \delta_k\delta_k\delta_k\}$ as $q_{sc}\mathcal{L} = 0$ whereas for an elastic continuum only $\delta_k\mathcal{L} = 0$. In an open system ultra-high tensile forces envelop any matter different from elastic fields. Particle clouds of large masses are generated by quadratic in mass iterated forces. Measured diurnal variations of ion concentrations as well as seasonal variations of CR count rates confirm a quantum entangled superfluid universe in Section 10. FZU resolves CCP, QE as well DM by a bifurcating spacetime supposing k-component pseudo-congruences [2] [7]. The origin of QE is a k-component pseudo-congruent curvature as an alternating current between capacitor-like layers. The heat energy gain arises from superfluid layer-temperature vs. altitude-entropy changes as a Carnot process in Section 9. The origin of charge and mass by Feigenbaum renormalization using Hieb's hypothesis is an open problem [8] [9]. Hieb's conjecture $2\pi\delta_F^2 \simeq \alpha_f^{-1}$ already had accuracy 9×10^{-4} with Feigenbaum constant δ_F and fine structure constant α_f which is refinable on entropy-surface-area $4\pi R^2 \simeq g_1^{:9n}$ by optimizing $g_1 + \cdots + g_n$ [10] [11]. Vacuum energy ρ_{vac} in quantum statistics (QS) ρ_{QS} is hundreds of orders of magnitude greater than the experimental value ρ_{exp} (CCP) [6] [12]. Contrary, QS measures QE as a spooky action at distance. However, high-precision nanostructure measurements are in good agreement with QS. DM requires a $\boldsymbol{B}$-field line pole in the complex electromagnetic field $\boldsymbol{E} + i\boldsymbol{B}$ realized e.g. by a ball of segments as a large cloud (monopole) mass where the quadratic in mass interaction dominates over linear rest mass [5]. The aim of the present note is to describe meV semiconductor experiments to clarify both fundamental problems. Charge quanta are experimentally detected for a mass ratio 10^{20} between oil drop and electron [13]. In bifurcating spacetime of FZU the Millikan experiment (ME), the quantum Hall (QH) effect, atmospheric clouds and universe clouds are shown to be self-similar tight-binding models each of mass ratio of about 10^{20} extending Dirac's large number hypothesis [2] [14]. A liquid state tight-binding approach is capable to explain QH [15]. A charge of small mass m_e floats in a quasi-homogeneous large background cloud mass M_p. Accordingly, a QH tight-binding model with Born-Oppenheimer parameter κ_{BO} of accuracy $\kappa_{BO} = 10^{-5}$ requires a thermal background cloud of Planck mass $M_p \simeq 10^{-5}$ g [2]. Surprisingly, atmospheric clouds move with similar mass ratio with respect to earth mass. Mass ratios of universe mass $M_u \simeq 10^{56}$ g to that of solar system 10^{33} g (10^{24}), atmospheric clouds of mass 10^8 g of volume 10^9 m^3 with density 0.5 g·m^{-3} to earth mass of 10^{27} g (10^{19}), ME oil drop of mass 10^{-12} g to electron mass 10^{-30} g (10^{18}) are set to κ_{BO}^4. Opposed is a liquid cloud slushy mass 10^{-5} g surrounding an electron mass 10^{-30} g (10^{25}) as a correlated thermal potential V_T of path-ordered, non-dissipative, non-radiative flow lines giving $\kappa_{BO} = 10^{-5}$ whereas $\kappa_{BO} = 10^{-3}$ at ME. A mass ratio of wood of 3×10^6 g to leaf mass of 3×10^4 g is 10^2 giving an uncertainty of about 0.3. The Enhanced Vegetation Index (EVI) of plant growth displays plateaus between 0.2 and 0.6 for a 120-day cycle in [16]. Orbits of period-doubling k-components of a quadratic map alternate with a lap number l_ω of equivalent periods ω. Simplest cycles q_{sc} of iterated quadruples $k+3 \in \{k, k+1, k+2\}$ yield a bicubic bi spinor norm solving CCP. Nanostructure experiments and cosmological and global parameter are self-similar [2]. In Section 2 physical scales are introduced in the quadratic map of dimensionless curvature. Section 3 relates multi-dimensional action functionals to one-dimensional complex holomorphic functions like the Dirichlet L-function or $\xi(z)$. The physical motivation is that a closed one-dimensional complex contour is a curvature or time-thermal Carnot cycle as a base for stress-energy stability. Section 4 confirms Feynman diagram series for all interaction which are based on the simplest cycles of iterated curvature. In Section 6 equivalence between the quadratic map and invariant substitutions of a quartic polynomial of curvature is seen in context of Friedmann equations. Inducible CR-emission is predicted by transitions between conductivity plateaus in QH in Section 7. QH plateaus are described as holomorphic leaves of a growing tree generating non-reversible Carnot cyclic clouds with quadratic-in-mass van der Waals-like interaction.

2. Unified Field Equations as the Simplest Cycles

The quadratic map based FZU implies Lorentz-invariance by complex fixpoints of binary invariant substitutions $\gamma(\phi_3)$. In Hermite variables the universe radius $R_u = H(\phi_4)/48\phi_4$ enters the time integral of the Friedmann solution [17]

$$ct = \int \frac{\sqrt{R_u}\,\mathrm{d}R_u}{\sqrt{\phi_3(R_u)}} \tag{1}$$

with Hessian $H(\phi_4)$ of a quartic polynomial ϕ_4 with $\Phi_n(t) = \sum_{i=0}^{n} a_i t^{n-i}$. A cubic invariant polynomial $\phi_3(R_u)$ implies discriminant changes $\Delta_3 \to \Delta_3\phi_3^2$ under $\gamma(\phi_3)$ with $4H^3(\phi_3) + Q^2(\phi_3) + 27\Delta_3\phi_3^2 = 0$ for invariant $Q(\phi_3) \simeq g_3$, $H(\phi_3) \simeq g_2$. In FZU, the simplest cycle quadruples $q = \{1, \delta_k, \delta_k\delta_k, \delta_k\delta_k\delta_k\}$ are one addition step k, $k+1$, $k+2$ on elliptic curves with a linear relation between three polynomial coefficients a_i. This is equivalent to the singular case of a normal bicubic field $\mathbb{N}\left[\sqrt{\Delta_2}\right] = \mathbb{K}[\partial]\mathbb{K}'[\partial]\mathbb{K}''[\partial]$ with a square discriminant of a quadratic field $\Delta_2 = \square$. Discriminants $\Delta_n = \Delta_2 = \Delta_3 = \Delta_4$ are the $n^2 \cdot n^2$ dimensional determinant $q = (\hat{a} \otimes I - I \otimes \hat{a})^2$ [18]. This holds for a linear relation $a_{ij} - a_{i'j'} - a_{i''j''} = 0$ between three coefficients of $\sqrt{q}$, e.g. for $n = 2$

$$\sqrt{q_{ij}} = \begin{vmatrix} 0 & -a_{12} & -a_{12} & 0 \\ -a_{21} & a_{11} - a_{22} & 0 & a_{12} \\ a_{21} & 0 & a_{22} - a_{11} & -a_{12} \\ 0 & a_{21} & -a_{21} & 0 \end{vmatrix} \tag{2}$$

$\sqrt{q}$ is singular if $a_{11} - a_{22} - a_{12} = 0$. A three-component linear relation (10) appears for a quadruple of shifts $q = \{1, \delta_k, \delta_k\delta_k, \delta_k\delta_k\delta_k\}$. A linear sequence $c_k a_k + c_{k+1}a_{k+1} + c_{k+2}a_{k+2} = 0$ enters a local process. This q_{sc} linear relation between three functionals holds e.g. for general relativity. Here $a_{ij} \simeq R, \Lambda, T$ imply the linear relation $4\Lambda - R = \kappa_4 T$ taking the trace in Einstein field equations $R_{\mu\nu} - 1/2 g_{\mu\nu}R +$

$\Lambda g_{\mu\nu} = \kappa_4 T_{\mu\nu}$. Again, Dyson equation for Greens function G, mass operator Σ with $a_{ij} \in \{G, G_0, \Sigma\}$ and Bethe-Salpeter equation with $a_{ij} \in \{P, P_0, \Xi\}$ for polarization P, P_0 and vertex part Ξ are linear in three irreducible functionals [19]. In distinction, Feigenbaum renormalization $-\alpha_F z_{2k} = z_k$ is global where α_F acts as a generator. A complex quadratic map $\gamma \circ R$ of universe radius or curvature is proportional to a product of Green's functions as shown in Sections 6 and 7. Feynman diagram series hold for unified fields for open, closed or flat spacetime in FZU. The Lebesgue measure in the time integral (1) reflects chaotic bifurcations in a complex global potential $t + i\beta \simeq V + iV_T \simeq \omega$ in Equation (13).

3. Mass, Energy in a Dimensionless Information-Based Universe

Information currents depend on binary substitutions $\gamma(\phi_3)$ which are symbolic linear but quadratic maps. Complex γ-fixpoints are viewed as Lorentz-transformations giving rational coordinates. Modular and elliptic invariants $j(\omega)$, $\gamma_2(\omega)$, $\gamma_3(\omega)$ depend on $f(\omega)$. A Lorentz invariant $f(\omega)$ is a mass for powers f^3, f^8, f^{12} and f^{24}. The Legendre modular function $\lambda_\mu = \lambda_{\mu m}/m + 1/2$ gives e.g. a mass $m = 4/f^{12}(\omega)$ where $\lambda^2 - 1/4 = m^2$. The Dirac-like current density $\lambda_{\mu m} = \bar{\psi}_q \lambda_{\mu m q q'} \psi_{q'}$ is invariant for equivalent substitutions of periods ω which are called laps l_ω. Period-doubling bifurcating k-components of γ generate a tree of masses. Iterating the Weber invariant $f(\omega)$ is iterating over all possible masses in an universe. An iteration is like a quadratic transformation of periods ω where the Legendre modular function λ proportional to a coupling constant $\lambda \simeq G_w \to 0$ of invariances $\lambda, 1/\lambda, 1-1/\lambda, 1/(1-\lambda), \lambda/(1-\lambda), 1-\lambda$. The zero-energy-universe with q_{sc} cycles is equivalent to self-similar four steps leading to gravitational waves [20]. In FZU energy is gained by q_{sc} being thermal Carnot cycles. A quadratic in mass (moment of inertia, quadrupole moment Q) expansion transforms a Lorentz-invariant tree into resting, floating masses by the algorithm

(*fixpoints of* γ) $\to \gamma$ (*Lorentz-invariant*) $\to q_{sc} \to \psi_s \to Q_{ij}$ (*three-dimensional resting* $\boldsymbol{v} \to 0$)

Pair creation rest mass energy is overwhelmed by a quadratic van-der-Waals-like potential in the limit of an infinite number of quadrupolar constituents being momenta of inertia. Unobservable ultra-high energy particles above GZK cutoff are identified with k-components between tree root in z_{nt} and first v_{Sh} at $k = 3$. Doubling at logistic parameter $r \simeq 3.54 \simeq 4$ suggest a base 4 Fermat number transform. All k-components imply invariant elliptic addition steps with $\lambda g^2 \simeq G_w M_w^2 \simeq G_w H_w^{-2} \simeq inv$ with modular unit g, Hubble parameter $H_w = \delta_k \ln\varphi$, order parameter $\varphi \simeq K + iK'$, quarter periods K, K', cloud masses $M_w \simeq g$ and coupling constants (6). Interacting shells $w = 1, 2, 3, 4, 5$ *are* invariant plateaus $M_w \simeq H_w^{-1}$, *i.e.* $M_5 > \cdots > M_1$ with

$$\rho_{vac} \simeq \frac{H_w^2}{8\pi G_w} \simeq \frac{H_4^2}{\kappa_4 c_l^2} \simeq \hbar c_l \simeq inv, \kappa_w \simeq \frac{8\pi G_w}{c_l^4}$$

Invariant addition despite fluctuating elliptic curves in spacetime solves the cosmological constant problem with a w-independent mean vacuum density ρ_{vac}. Because the Hubble parameter H_w depends on k-components as $\ln 2^{2^k}$ the third branch $k = 3$ yields a mean CMB energy density

$$\rho_{vac}^{CMB} \to \frac{H_5^2}{8\pi G_5 \left(2^{2^3}\right)^2} \simeq \frac{\rho_{vac}}{2^4} \simeq \rho_{vac}^{CMB}\left(T \simeq 2.3\ \mathrm{K}\right)$$

The relation between iterates, curvature and field tensor drawn in Section 7 allows to associate tree root k-components with CMB waves where periods ν_{Sh} act as an external alternating current. A dimensionless bifurcated spacetime concludes to 3 K CMB of wavelength 1…10 cm or frequency 1…10^3 GHz because k-components fill out spacetime nearly isotropic [21].

4. L-Function Regulator Process

Fluid dynamics in Section 6 is reducible to one complex dimension near zeros of a holomorphic function $\xi(z \simeq \lambda)$. Cyclotomic Kronecker-Weber extensions of a bicubic field are the origin for spacetime points by a bifurcating k-component spacetime tree. Invariance $\gamma\circ\xi$ and $\gamma\circ z$ in $\xi(z = \lambda[f(\omega)])$ covers λ while iterating the modular invariant $\gamma\circ f(\omega)$. Note that $f_k^{24} \simeq 1/\lambda\lambda'$ is singular in λ where $z \simeq \lambda$. Simple $\zeta(z \simeq \lambda)$-poles are linked to simple $\zeta(z)$-zeros by a certain different substitution $\gamma\circ z_{nt}$ which is regarded as a mass operator expansion. A holomorphic $\xi(z = \lambda[f(\omega)])$ in λ depends on curvature tensor $f(\omega) \simeq R_{\mu\nu} \simeq \boldsymbol{E}$ where $\xi(z = \lambda[f(\omega)]) \simeq \boldsymbol{E}$. Dedekind zeta function $\zeta(z, \mathbb{K})$, Riemann zeta function $\zeta(z)$, ξ-function and Dirichlet L-function $L(z, \chi)$ satisfy

$$\frac{\zeta(z,\mathbb{K})}{\zeta(z)} = \frac{\Gamma(z/2)\, z(z-1)\,\zeta(z,\mathbb{K})}{2\pi^{z/2}\xi(z)} = L(z,\chi) \tag{3}$$

where $L(z,\chi) \simeq R_\Delta/\sqrt{\Delta}$ is proportional to a regulator $R_\Delta = R_{\Delta ij} = \ln_b E_{ij}$, for base b, fundamental unit E_{ij} and discriminant Δ of a cubic field. In iterates of $z \simeq \lambda$ variable z_k is $f(\omega)$-like and z_{k+1} is λ-like. Extension fields with r-dimensional lattices of cyclotomic units E_{ij} ($1 \le i, j \le r$) induce local minima of the L-function. A screened Poisson Equation (4) couples via Equation (3) with Dirichlet-character χ conveyed through chaotic periods to the Artin L-function and Dedekind zeta function $\zeta(z, \mathbb{K})$. The present approach opens a calculation of field Lagrangians by Epstein zeta functions $\zeta\left(z, \mathbb{Q}\left[\sqrt{\Delta_k}\right]\right)$, hyperelliptic theta functions $\vartheta(u_\pm)$ and L-functions through a regulator index. The L-function in (3) depends on a module norm function which depends on a power of the Dedekind eta function $\eta(\omega)$ [22]. A function that is holomorphic throughout the finite plane is generally called an entire function, and a distinction is made between entire rational and entire transcendental functions, depending on whether their power series expansions have finite or infinite terms. A Hecke L-series is an L-series for a character on a group that is a generalization of both residue class and ideal class groups and is an entire transcendental function. The transformation of Hecke L-series into a linear combination of Epstein zeta functions shows that the quotient of the Dedekind zeta function $\zeta(z, \mathbb{K})/\zeta(z)$ can be extended holomorphically to the entire complex plane. The Dirichlet L-function $L(1, \chi)$ is proportional to a circulant matrix in $-h_\Delta R_\Delta / \sqrt{\Delta} = \left(12\ln 2 + \ln\lambda + \ln(1-\lambda)\right)/8\sqrt{\Delta} \simeq \left(12\ln 2 - \lambda + \ln\lambda\right)/8\sqrt{\Delta}$. For optimal units $f \to f + \ln f$ the L-function $L(1, \chi)$ is proportional to a coupling constant and to a mass. A regulator process is proposed as a stationary cycle $R_\Delta \simeq \mathcal{L}$ which takes lower values than that for a given extension field [3]. Rational (real) coordinates imply a vanishing discriminant $\Delta \to 0$ (general relativity). To determine rational fields $\Delta = 0$ is a highly nonlinear process by the Minkowski bound prescribing $\Delta \to \infty$ for cyclotomic limits. Two stripes $\pm 1/2 \pm im_n$ in a holomorphic entire function $\xi(z)$ yield a Poisson-like equation for λ-slices as two capacitor plates

$$Q(z) = \Delta_{xy}\left(L(z,\chi)\xi(z)\right) + \mu_s L(z,\chi)\xi(z) = \pm\mu_c\left(Im\lambda \pm m_n\right) \tag{4}$$

Conductivity plateaus of the holomorph functions $\xi(z) \simeq \boldsymbol{E}$ with $z \simeq \lambda$ [$\gamma \circ f$] satisfy the hyperbolic Laplacian $\Delta_h \xi(z) = 0$ with $\Delta_h = y^2\Delta_{xy} = \mathrm{Im}\lambda^2\Delta_{xy}$. An electric field-like $\xi(z)$ is subjected to a λ-process as external current. Lagrange condition (μ_s) is a nontrivial $\xi(z_{nt} = \pm 1/2 \pm im_n) = 0$ as a screening process. Lagrange condition (μ_c) is a finite charge to-mass ratio because λ depends on mass. Solutions $Q(z)$ are modified Bessel functions which are entire functions. Four zeros $Q(z \simeq z_{nt} = \pm 1/2 \pm im_n)$ are related to a quadruple q_{sc} of steps. Gravitational waves are one-dimensional waves in four-dimensions [20] [21]. The first $Q(z)$ iterate is a fourth-order differential equation $a\Delta_h + b\Delta_h\Delta_h = 0$ known from [23]. Subsequent iterations yield 2^{2^k} polar entire iterates $Q(z)\circ\ldots\circ Q(z)$ solving Δ_h. Iterates $\gamma \circ z$ yield a 2^{2^k}-order differential equation. This screened two-dimensional Poisson equation is invariant with respect to a simultaneous change $\gamma \circ z \simeq \gamma \circ \lambda$ and $\gamma \circ z_{nt}$. Zeros z_{nt} are certain values of the Legendre modular function λ where $\gamma \circ \lambda$ implies a quadratic equation for masses m_{nt}. This quadratic equation for masses leaves Kummer surfaces $K(X(\gamma \circ f(\omega)))$ invariant. Here $\gamma \circ f$ and $\gamma \circ z \in \mathbb{C}^w$ yield an underdetermined system of quadratic equations. A longitudinal, transverse and rotatory vicinity of an arbitrary point in a spherical-shell in $\mathbb{C}^w$ has surface, altitude and volume components. Shells can be explained by a capacitor model. Locally, zeros of $\zeta(z_{nt})$ in capacitor plates-stripes $\pm 1/2$ are condensation nuclei in five atmospheric spherical shells in $\mathbb{C}^w$. A permanent alternating current flow between capacitor plates due to seasonal and altitude variations is shown in **Figure 1**. The $L(z, \chi)$-function gets a non-equilibrium regulator process with three constituents μ_1, μ_2, μ_3 in Equation (14) under subsequent z-maps. μ_1, μ_2, μ_3 are a conductivity plateau (holomorphic equilibrium state), air ionization (net rate) and CR bifurcation (scattering). The regulator term μ_1 is an entire, holomorphic conductivity plateau. The term μ_2 is a count rate which is a non-equilibrium air ionization rate proportional to a statistical occupation being the geometric zeta function $\zeta(l_s, m_s, z)$. The third term μ_3 is a scattering rate of occupation number changes as a bifurcation tree. Here k-components explain as well CMB and ultra-high CR shower. Inherent in any definition of a spacetime point is the uniqueness and invertibility which requires simple zeros z_{nt} of a complex holomorphic function. Multiple of z_{nt} are charge quanta which arise in pairs. Globally, a seasonal average counts the number of k-components as the number of particles as leaves of a tree. Locally, capacitor plates obey congruent alternating voltages $\mod\left(2^{2^k}-1\right)$ which explains the phenomenon of QE. The congruence is due to a renormalized Feigenbaum Equation (9) where a second constant α_F proves the existence of a generator. Zeros z_{nt} are a singularity in the r.h.s of Equation (4) as an alternating current for equivalent laps $\lambda(\gamma\circ f) = \lambda(f)$.

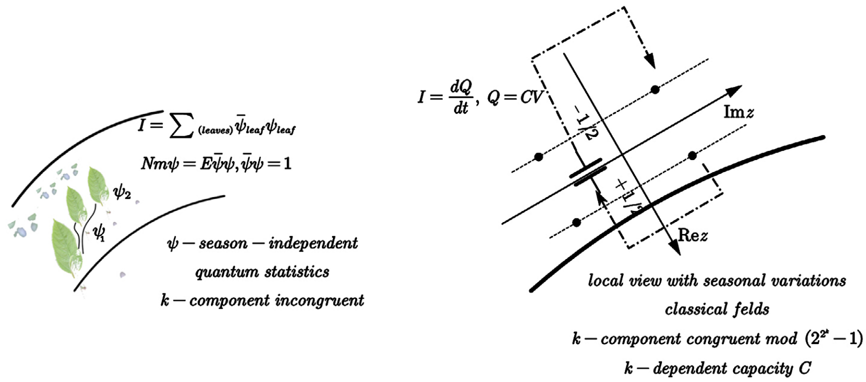

Figure 1. A second sound in quadrupole interacting z_{nt}: (Left) Long-wave (seasonal) motion; (Right) Short-wave motion with two stripes $z_{nt} = \pm 1/2 \pm im_n$ of the Riemann zeta function where stripes ±1/2 are viewed as capacitor plates.

A first and second sound in **Figure 1** corresponds to a growing global binary tree of particles (leaves in seasonal variation) superimposed by local capacitor voltages as a CR-shower. Spacetime forms from a Carnot cycle of longitudinal, transverse and rotatory directions. In plant growth the EVI displays plateaus [16]. A charge in Equation (4) is the $k \to \infty$ limit of holomorphic leaves (plateaus) of neutral chaotic quadrupolar γ-simplest cycles in $\xi(z)$. The QH current is a neutral oscillating complex quadrupole (inertial) moment Q_{xy}. Experimental support for FZU is oscillation of the gradient of global temperature over 10^8 years (=plateaus of temperature) and microwave emission at QH [24] [25]. Detector dimensions for ME, QH and CR detector (Wulf's bifilar electrometer, Wilson chamber) as well air ionization (Gerdien condenser) are comparable [26]. FZU predicts an invariant dimensionless vacuum energy density $\rho_{FZU} \simeq \lambda_k g_k^2 \simeq \rho_{exp}$ for cycles by a power tower of modular units g_k. Transitions between conductivity plateaus σ_H (leaf growth) induce CR emissions. The tight-binding model with $\kappa_{BO} \simeq 10^{-20\times 1/4} = 10^{-5}$ of mass ratio 10^{20} displays potential changes as relative mass changes. A first prediction of high-energy emission at QH not yet observed is extended to a model of a universal CR-atmospheric charge cloud superfluid [27] [28]. Iterated Weber invariants $f(\omega)$ by map (10) is regarded as a complex curvature which is proven in Section 7. Doubly-periodic cycles ν_{Sh} due to Sharkovskii's theorem require two constants α_F, δ_F. Whereas laps l_ω are stationary particle orbits k-components are a bifurcating shower of particles. Particles at first periods ν_{Sh} at $k \le 3$ are not observable. Periods ν_{Sh} near $k = 3$ is spacetime oscillation felt as cosmic microwave background (CMB). k-components changes into a fluid of elastic spacetime at step k

$\simeq G_5^{-1}$ with dark exchange scattering coupling constant $G_5 \simeq 10^{-167}$. The most general Riemann surface $1/2w(w+1) < 3w+3$ for $w \le 5$ induces a self-similar pseudo-congruence for $k \simeq 2^{2^9}, 2^{2^{10}} \to 1$. Coupling constant G_w in the regulator index intersects with Legendre module $\lambda_k = 4\boldsymbol{q}^{2^{k-1}}$. Here period-doubling $\omega_k \to \omega_{k+1} + \omega_{k+2}$ as $\omega \to 2\omega$ gives a tower of the nome $\boldsymbol{q}^{i\pi\omega} = \mathrm{e}^{-\pi K'/K} \simeq 2$ like a second Feigenbaum constant α_F. FZU-emission rates of CMB at QH behave as κ_{BO}^{-2}. Regarding k-components as identical charges QS overestimates $\rho_{\exp}$ by factor $2^{2^k} \simeq G_5^{-1}$ as a F_9, F_{10}-congruences with Fermat number F_t in $\rho_{\mathrm{QS}} \gg \rho_{\exp}$ [29].

5. Feynman Diagram Series for Five Interactions

A bi spinor ψ is defined as a simplest cycle quadruple of norm ($\Sigma_{(q)} E_q^{-2}$) = $\Sigma_{(s)} \psi_s \bar{\psi}_s$ averaged over laps l_ω which remains valid for all interactions w. QS sets a norm $\Sigma_{(s)} \psi_s \bar{\psi}_s = 1$ for all bifurcating 2^{2^k}-CR air shower components which overestimates vacuum energy ρ_{vac} by the CCP-factor 2^{2^k}. ρ_{exp} contains only rare ultra-high CR counts. FZU consists of cryptographic-like pseudo-random integer addition steps on fluctuating elliptic curves. QS implies finite λ_k and g_k. Macrostructures imply $\lambda_k \to 0$ and large $g_k \to \infty$ for $k \to \infty$. Self-similarity implies invariance $\lambda, 1/\lambda, 1-1/\lambda, 1/(1-\lambda), \lambda/(1-\lambda), 1-\lambda$. On the most general complex Riemann surface the cubic behavior of $f(\omega)$ transmits to λ and the coupling constant G_w for $w \le 5$ interactions $w = (1 - 5) = (strong, weak, em, grav, dark)$. A bicubic bi spinor norm $Nm(\psi) = E_i \psi' \psi'' = 1$ of conjugated units is capable to formulate an invariant energy density

$$\rho \simeq \frac{1}{2} \Sigma_{(w,\boldsymbol{k})} G_w(E) E(\boldsymbol{k}) \simeq \rho_{FZU} \simeq \rho_{exp} \simeq 10^0 \cdots 10^{-1}\,\mathrm{eV} \cdot \mathrm{cm}^{-3} \simeq \rho_{CR} \simeq \rho_{CMB} \quad (5)$$

FZU dimensionless energy $E(\boldsymbol{k})$ is defined as a change of units E_i or a change of λ_k related to k-components [2]. λ_k defines a Dirac equation where the wave vector $\boldsymbol{k}$ is related to periods ν_{Sh} capturing Bloch states by $\gamma(\phi_3)$-fixed points. CCP requires a cutoff for $E(\boldsymbol{k} \to \infty) \to \infty$. QS implies ν_{Sh} congruent laps l_ω and k-incongruent components. FZU implies finite $E(\boldsymbol{k} \to \infty) \to E_\infty$ and predicts a congruence $2^{2^k} \to 1$ which lowers the vacuum energy. A coupling constant

$$\ln G_w(0) = -w! 2^w \ln_3^w 2 \quad (6)$$

results from a formerly constant regulator index $R_{\Delta ij} = \ln_b E_{ij}$ in Equation (14) optimized by circulant process. For dark matter at $w = 5$ one has $G_5 \simeq 10^{-167}$. In QS the circulant behavior is reflected by a scattering process. For simplest cycles q_{sc} the Euclidean norm ($\Sigma_{(q)} E_q^{-2}$) = $\Sigma_{(s)} \psi_s \bar{\psi}_s$ in Equation (4) recovers the until now accepted bi spinor norm. The cutoff in Equation (5) is due to Equation (6) with energy-dependent coupling constant $G_w(E)$. Local minima of the L-function are stationary states. In macrophysics the unified bi spinor norm is a tidal-like state of four curvatures of four points. CCP is a time averaging problem for rare but ultra-large mass $M_k \simeq g_k$ on bifurcating clouds

$$\rho_{QS} \simeq \delta_k t M_k c^2 R_{net} + \rho_{exp} \quad (7)$$

with mass $M_k \to \infty$ and $R_{net} \to 0$ depending on the four-dimensional volume of complex time $d\sigma_5$ for time interval $\delta_k t \to \infty$. Number theoretic congruences $1 = 2^{2^k} \simeq G_5^{-1}$ resolve CCP by reducing ρ_{QS} to ρ_{exp}. As a result, CR and CMB occur in any bifurcating spacetime also at low altitude-atmospheric layers. In FZU the order parameter $\varphi \simeq K + iK'$ is linear expanded into complex curvature $R \simeq f(\omega)$. Elliptic curves represent themselves a self-similar system because quarter periods K, K' are exact theta constants. Complex scalar curvature $R = \gamma \circ R_u$ produces bifurcating tensile forces as a perquisite for stationary spacetime or balanced ionized CR-CMB clouds. Iterated complex $f(\omega)$ enter theta constants $\eta(\omega) f^2(\omega)$ which are equivalent to a correlated path-ordered complex temperature potential $V + iV_T$. Enveloping periods ν_{Sh} are explained by congruent integers a_k, b_k, Δ_k determining half-periods $\omega_i = 1/2\left(a_k + b_k i\sqrt{\Delta_k}\right)$ [2]. The most general Riemann surface includes added points on iterated elliptic curves as cryptographic, regular, pseudo-random chaotic period-doubling. Cubic roots $f(\omega)$ of $\phi_3(f(\omega))$ are iterated by

$$\gamma\left(\phi_3\left(f\right)\right) = \begin{vmatrix} \frac{1}{3}\phi_3'\left(f\right) & \phi_3\left(t\right) - \frac{f}{3}\phi_3'\left(f\right) \\ -1 & f \end{vmatrix} \tag{8}$$

In the context of the symbolic map (8) an orbit subgroup of equivalent lattices with $\det\gamma = 1$ is called lap I_ω of γ else a k-component. Laps I_ω as non-turbulent Carnot cycles ν_{Sh} of the thermal potential $V + iV_T$ accumulate a large neutral background cloud. This is enabled by quadratic-in-mass-excitations of large scale floating non-radiative bifurcations as a pre-stage of spacetime from a zero of a complex entire, differentiable function. The electric field-like holomorphic function $\xi \simeq \boldsymbol{E}$

$$\xi\left(z\right) = \left(\frac{z}{2}\right)\pi^{-\frac{z}{2}}\Gamma\left(\frac{z}{2}\right)\zeta\left(z\right) = \frac{1}{2}\prod_n\left(1 - \frac{z}{z_n}\right) = -\frac{\partial j\left(z\right)}{\partial z}$$

is governed current-like

$$j\left(z\right) = -4\int_1^\infty \frac{\mathrm{d}t}{\log t} t^{-1/4}\partial_t\left(t^{3/2}\partial_t\left(\vartheta_3\left(0, \mathrm{e}^{-\pi t}\right) - 1\right)\right)\sinh\left(\frac{1}{2}\left(z - \frac{1}{2}\right)\right)\log t$$

with Jacobi theta function ϑ_3 [30]. Driven by $\gamma \circ f(\omega_k)$ and invariances $\gamma \circ z$, $\gamma \circ \xi(z)$, $j(z)$ is a universal clock frequency in Equation (4). Like zeros $z_{nt} = \lambda_k$ as quanta of charge Coulomb singularities appear for $f(\omega_k)$ $[\lambda_{k+1}]$ generalizable to n-dimensions [21] [31].

6. Binary Invariant Neutral Superfluid Potential Flow

A relation of charge and flux to thermal convection has already been proven. The superconducting order parameter φ is a theta function [32]. Nonequilibrium electrons in semiconductors are capable for Benard convection [33]. Fluid dynamics $\boldsymbol{X}_{k+1} = \hat{a}_Y[\gamma]\boldsymbol{X}_k$, $\boldsymbol{X}_{k+2} = \hat{a}_X[\gamma]\boldsymbol{X}_{k+1} \in \mathbb{R}^3$ on $K(X(f) = (1, -f, f^2, 1))$, $W(Y(f) = 1, -f, f^2, -f^3)) \in \mathbb{P}^3$ is governed by two different SE (3) steps for $\gamma(\phi_3) \circ f(\omega)$ with orthogonal transformation $\hat{a}_X[\gamma(f)]$, $\hat{a}_Y[\gamma(f)]$. Discrete ideal fluid dynamics consists in iterating singular 4×4 matrices for Kummer and Weddle surfaces $K(X)$, $W(Y)$. Kirchhoff equations for body and fluid positions are the continuous limit of $X(f)$ and

$Y(f)$ iterates. Iterated velocities $\boldsymbol{X}_{k+1}(f(\omega)) - \boldsymbol{X}_k(f(\omega)) = \nabla V_T$ describe a non-turbulent flow with potential (13). Map (8) creates an entire, holomorphic polynomial $f_k(f_{k=0})$ in $f_{k=0}$ which is singular in dependence on λ. At step $k = 0$ a pole $f^4(\omega)|_{k=0} = 2^4/\lambda(\lambda - 1)$ exists on λ-plane of $\zeta(z = \lambda)$. Subsequent steps yield Feigenbaum renormalized invariants

$$z_k = -\alpha_F z_{2k} \leftrightarrow \gamma^{(\mathrm{ren})}(z) = -\alpha_F \gamma^{(\mathrm{ren})} \circ \gamma^{(\mathrm{ren})}(-z/\alpha_F) \quad (9)$$

$$c_k z_k + c_{k+1} z_{k+1} + c_{k+2} z_{k+2} = 0 \leftrightarrow \gamma^{(\mathrm{ren})} = \gamma + \gamma \circ \Gamma^{(\mathrm{ren})} \circ \gamma^{(\mathrm{ren})} \quad (10)$$

$$F(t,z) = \gamma(\phi_3(t)) \circ z \simeq \phi_3(t)/(t-z) - \frac{1}{3}\phi_3'(t) \quad (11)$$

$$F(t,z) \simeq A_\mu G_{ss''} \gamma^\mu_{s''s'''} G_{s'''s'} - \frac{1}{3} \frac{\delta A_\mu}{\delta\left(G_{ss''}\gamma^\mu_{s''s'''}G_{s'''s'}\right)^{-1}} \quad (12)$$

Accordingly, binary substitutions γ envelope Feynman diagram series of Dyson-like equation for a Greens function $G_{ss}[\psi]$ defined in terms of a quartic roots shifted to $s = \pm\infty, \pm i\infty$ as q_{sc} [3] [29]. Optimal units $E(\omega_k)$ and $f_k = f(\omega_k)$ with Euclidean norm $\sum_q f_q^{-2} = \sum_q f_q' f_q''$ reproduce a bicubic spinor norm $\mathrm{Nm}(f(\omega)) = f(\omega)f'(\omega)f''(\omega) = 2$ with complex conjugates invariants f' and f''. Quantum statistics implies k-incongruent γ-orbits averaged over stable laps l_ω (seasons) in a binary tree. Equation (10) is solved by a tent map giving e.g. a Cantor set $\zeta(l_s, m_s, z)$ and in the limit $k \to \infty$ a complex Lebesgue measure $\mathrm{d}l_{xy}$

$$V_{T_{global}} = \int \nabla V_{T_{cloud}} \mathrm{d}l_{xy} \quad (13)$$

The complex line element $\mathrm{d}l_{xy} \leftrightarrow \mathrm{d}u = \mathrm{d}z/\sqrt{\phi_3} \leftrightarrow \gamma \circ \mathrm{d}z/\sqrt{\phi_3}$ is iterated by Equations (9)-(12). A high voltage measured between points on a straight line is resolved on a fractal line. Optimal entropy is given by minimizing the quadratic form of a circulant regulator $R_{\Delta ij}$ for finite geometric zeta function $\zeta(l_s, m_s, z)$ of string length l_s and multiplicity m_s and Euclidean norm $N(E) = (\Sigma_{(q)} E_q^{-2}) = \Sigma_{(s)} \psi_s \bar{\psi}_s$ as

$$2\mu_1 R_{\Delta ij} + 2\mu_2 \zeta(l_s, m_s, R_{\Delta ij}) \mathrm{e}^{2R_{\Delta ij}} + \mu_3 N(\mathrm{e}^{R_{\Delta ij}}) \zeta'(l_s, m_s, R_{\Delta ij}) = 0 \quad (14)$$

for an entropy-based universe [10]. A Mandelbrot zoom sequence first unrelated explains the Huygens-Fresnel principle by μ_1, μ_2, μ_3 superposed cardioids and zoomed bulbs of spheres-in-spheres information currents [2]. Equation (14) is solvable in complex four-dimensional space by a four-component complex rotations of units $E_i = \exp(l_i)$. Local plateaus in (14) are $L(z, \chi)$-function induced elastic Lagrangians.

7. A Classical Bi Spinor

All forces are treated uniquely by Feynman diagrams for bi spinor $\psi_s \simeq f_s(\omega)$ with Euclidean norm $(\Sigma_{(q)} E_q^{-2}) = \Sigma_{(s)} \psi_s \bar{\psi}_s$. Bicubic q_{sc} in ψ_s is viewed as spacetime curvature $R_{\mu\nu} \simeq F_{\mu\nu} \simeq \boldsymbol{E}, \boldsymbol{B}$ governed by $z_{k+1} \leftarrow z_k^2 + c$ for $z \simeq f(\omega)$ rewritten as a quartic polynomial $\boldsymbol{R}_{\mu\nu}^4 + 2\mathcal{F}\boldsymbol{R}_{\mu\nu}^2 - \mathcal{G}^2 = 0$ with $\boldsymbol{R}_{\mu\nu} = Re z_k$, $\mathcal{F} = 1/2 Re(c - z_{k+1})$, $\mathcal{G} = 1/2 Im(c - z_{k+1})$. A finite iterated set z_k with periods ν_{Sh} can be projected onto complex plane as a generator g_k or a root of unity. Optimal coordinates appear in (14) for a tower $g_{k+1} \simeq \exp(ig_k)$ which interchanges wave vector and classical momentum as a classical particle. Universe anti-matter is defined as irreducible q_{sc} vertices 1, 2, 1'2' of a point as irreducible tidal motion [7].

8. Conductivity Plateau as a Holomorphic Leaf

A magnetic field $\boldsymbol{B} \simeq \delta_k h_t(g_k) \simeq$ (*days of the year*) is equivalent to changes of topological entropy $h_t(g_k)$ and seasonal changes as days of the year. Plant growth in units of EVI or conductivity at QH induced by gradient of temperature or electric field $\boldsymbol{E} \simeq \nabla T$ are comparable which is symbolically shown in **Figure 2**. A mass ratio 10^3 between wood and leaves yields accuracy 0.3. For $k \to \infty$ a universal coupling constant is expected resulting from an area $2\pi\delta_F^2$ corrected by a high-precision factor $g_1^{:9n}$ [8] [10]. The fine structure constant at high energies (high k values) exhibits a minimum e.g. 1/128 at 10^9 eV [34]. Similarly, a QH plateau describes a universal (all interaction containing) neutral quadrupolar current contained also in a definition of a bis spinor. Only a forest of trees with k-components of partial laps l_ω towards define a quantum of charge. The exosphere-earth-surface-capacitor state is a flowing congruent alternating current. The concept of charge is connected with alternating capacity changes of an ergodic treetop-root symmetry. The treetop-root system of the binary tree is asymmetric, non-ergodic, non-reversible and generates matter. This asymmetry is a quadrupolar-quadrupolar weak, nearly neutral capacitor state compatible with modular units and the Macdonald denominator formula. Here $\eta^{N(N-1)/2}$ is a product of theta functions $\prod_{1\le j<i\le N} \vartheta_1\left(u_i - u_j, \omega\right)$ which is a Vandermonde determinant Δ_N for the simple Lie algebra A_{N-1} [35] [36]. A Vandermonde determinant is $\exp(|u|^2)\Pi(u_i\text{-}u_j)^N \simeq \exp(|u|^2)\Delta_N$ which is known as the Laughlin-wave function similar to N^{th} order Weierstrass sigma functions $\sigma^{(N)}(u, \omega)$ for arguments $u = a\omega$ [37] [38]. Standard units of time and energy count the number of precessions n and the number of Carnot cycles m independent on fluctuating ω. A floating tidal-like phase-correlated bifurcating fluid cloud persists with balanced collision-less ionization in a stable universe. The minimum $z_k \simeq V_T(f_k)$ allows rare ultra-high energy CR and persistent CMB of the iterated 2^{2^k} polar holomorphic fluid $z_{k+N}\,[\ldots z_k]$ that forms a ball of string segments. A growing n-leaved tree as a 2^{2^k} quadrupolar ball due to a single zero z_{nt} opens the next zero point if all sites in $\mathbb{C}^5$ are occupied at $2^{2^k} \simeq G_w^{-1}$.

Figure 2. (left) Fractal zeta zeros in nature and nanostructure laboratory: Plant, green trees under blue sky and (right) Plateaus in quantized Hall conductivity [42] [43].

9. Second Sound Thermopower Cycle

The cosmic-ray-charge-cloud (atmospheric) model is a capacitor-like chaotic RC oscillator which stores charge and mass. The resistance R in the circuit is the k-component congruence, the capacity is the number of nontrivial zeros and its frequency are the number of cycles ν_{Sh}. The energy gain $VI \simeq V^2$ or $\simeq I^2 \simeq \delta_k h_t \delta_k T$ for voltage V and current I undergoes a quadratic map where the Carnot cycle area is $\delta_k h_t \delta_k T \det\gamma$. A one-dimensional zero of $\zeta(z_n) = 0$ is traversed by three-dimensional points $\boldsymbol{X}_k(t)$ of a dissipation less superfluid in space with electric field $\xi \simeq E(z) \simeq (\nabla V, \nabla V_T)$ composed from gradients of V and V_T. A closed loop in complex plane yields a holomorphic potential $V(z) = Q_S V_T(z)$ creates topological entropy h_t per charge carrier concentration N_e per z_{nt} via the Seebeck coefficient $Q_S = h_t/eN_e$. Physically a time-thermal Carnot cycle with two sounds (cycles) ν_{Sh} and q_{sc} yields a voltage (energy) gain up to ultra-high-energies over 2^{2^k} components for $k > 8$.

10. Global Seasonal Temperature Cycle and Local Altitude Entropy Cycle

First and second sound in a Carnot cycle gains energy where one-dimension extends to three dimensions as shown in Section 3. Exact addition on fractal chaotic elliptic curves implies a sound within a sound or $\nu_{\text{Sh}}[\nu_{\text{Sh}}]$ recursively. Waves of universe radius R_u are waves of temperature $R_u \simeq K, K' \simeq \vartheta$ and entropy h_t. Longitudinal, transverse and rotatory motions $\boldsymbol{k}_i\boldsymbol{k}_j$, δ_{ij}-$\boldsymbol{k}_i\boldsymbol{k}_j/k^2$, $\varepsilon_{ijkl}\boldsymbol{k}_k\boldsymbol{k}_l$ are global seasonal temperature waves and local altitude entropy waves where handedness creates spin. A spinor $\psi_q = f(\omega)[\lambda]f(\omega)$ has a simple pole $1/\lambda\lambda'$ for each multiple $f^{24}(\omega)$ entering the measure dl_{xy} in the global temperature potential (13). A holomorphic gradient $\nabla V_T \simeq E(z) \simeq \xi(z)$ in $\lambda_k[f_k(\omega)]$ gets singular in $f(\omega)$. A certain iterate $f(\omega)$ in $\lambda\lambda' = 2^4 / f^{24} = 1/4 - z_{nt}^2$ meets a zero z_{nt}. Four zeros $\pm 1/2 \pm im_n$ in V_T yield a three-dimensional quadrupole moment $r_i Q_{ij} r_j / r^5 \simeq 1/r^3$. The thermal potential $V_T(\lambda)$ has a cubic, roton-like upper valley: In dependence on defining the velocity of light $c_l = 1/\sqrt{\varepsilon\mu}$ by a vacuum permittivity $\varepsilon_0(r) \simeq r^2$ or not one gets $V_T(\lambda) \simeq Q/\varepsilon r \simeq Q/r^3 \simeq mr^2/r^3 \simeq m/r$ either a quadrupolar potential V_Q or a Kepler-Coulomb-potential in unified space. The Fourier-component of V_Q contains a contact interaction term giving a bag potential which is compatible with a cubic behavior of coupling-constants. Iterations $Q(z)\circ\ldots\circ Q(z)$ of the Poisson Equation (4) form a 2^{2^k} polar cloud of segments. Segments resolve e.g. fractal a 10^{20} eV voltage into a minimal e.g. 1 meV potential (13) and vice versa. The atmospheric equivalent of second sound is e.g. lightning bang and thunder as independent thermal and entropy cycles of q_{sc} of an incompressible superfluid. The cubic invariant couples longitudinal and rotatory components in roton-like upper energy valleys [39] [40]. The Feigenbaum diagram is a hysteresis of a Carnot cycle.

11. Cosmic Rays, Cosmological Redshift and Microwave Background in Bifurcating Spacetime

Dimensionless energy is scaled by k-components up to the GZK cutoff as the onset of first ν_{Sh}. [41]. A zero-energy-universe in the vicinity of every point is capable to create large cloud masses. Second sound is a quadrupolar wave inherent to spacetime as a background permeability $\varepsilon_0(\boldsymbol{k}) = 1/I_{ij}\boldsymbol{k}_i\boldsymbol{k}_j$. The potential $1/\varepsilon(\boldsymbol{k})\boldsymbol{k}^2$ corresponds to exchange scattering or permanent tidal waves of two objects. Its spatial dependence in $\varepsilon_0\left(R_u\right) \simeq R_u^2$ explains the cosmological redshift. CMB is caused by the overall first appearance of ν_{Sh} in clock rate $j(z)$. CR emissions have low count rate $1/2^{2^k}$ but ultra-high energy. So far organic matter has been used for power plants. An associated CR generation causing air ionization has been ignored so far which could be controlled in nanostructures as a novel possible future energy technology. Its energy gain can be estimated by the T-h_t hysteresis area of Carnot cycles. Besides understanding climate, second sound is implicit in a model of a universe and concerns background susceptibilities with apparent expansion and redshift.

12. Comparison with Existing Experimental Data

Rare CR of probability 2^{-2^k} are set in context to enhanced anomalous atmospheric ionization (μ_2-term), a changed air composition, nuclear disintegration stars in QH layers or plants. As a prerequisite for mass creation correlations over macroscopic dimensions in large scale CR detector arrays with a very low count rate up to 10^{-2} year are also a measure of stability. This holds also for organic matter where air ionization accompanies plant growth because of a partial small amount of matter created from nothing or matter canceled out by its negative field energy. Dimensionless Q_{xy} oscillations in Equation (4) are rather waves of the metric (gravitational waves). In form of CMB they indicate the stability of space. Accordingly, besides existing matter at plant growth matter plus radiation is created. The overall CMB is viewed as the part of first k-component cycles of bifurcating spacetime. A measured seasonal variation of CR counts confirms coupling to organic matter and atmospheric clouds in **Figure 3** as well as an associated measured seasonal variation of Be activity concentration in the air in **Figure 4**. FZU supposes an oscillating creation of matter by zeta zeros as zero-energy-universes. The velocity of the second sound is proportional to the entropy $\delta_k h_t \simeq \boldsymbol{B}$ and depends e.g. on magnetic field. QH microwave emission has been already detected **[25]**. A diurnal air ionization in vegetation areas has been detected in **Figure 5** which is classified corresponding to **Figure 2**. The present paper attributes this phenomenon to a finite CR generation with low count rate at plant growth. As an indication low k-components $k \simeq 1$ is capable to explain the CMB amount of 10^{-4} on vacuum energy ρ_{vac}. With increasing density of chaotic k-components quadratic and higher polynomial mass terms dominate the linear rest mass favoring growth of surrounding clouds or leaves. FZU favors creating large mass clouds near a nontrivial zero z_{nt} in distinction to a single-particle-big-bang-scenario. In FZU, existing particles serve as catalysts of an eternal non-equilibrium process or alternating capacitor state. Various experiments support FZU which have been previously classified differently. These include microwave emission at quantized conductivities, seasonal variations of cosmic-ray intensity and diurnal variations of air ion concentrations in different vegetation areas. First-sound entropy-changes of k-congruences and second-sound temperature-variations yield an oscillation of a temperature potential (13) over a fractal line dl_{xy} in natural history as shown in Figure 6.

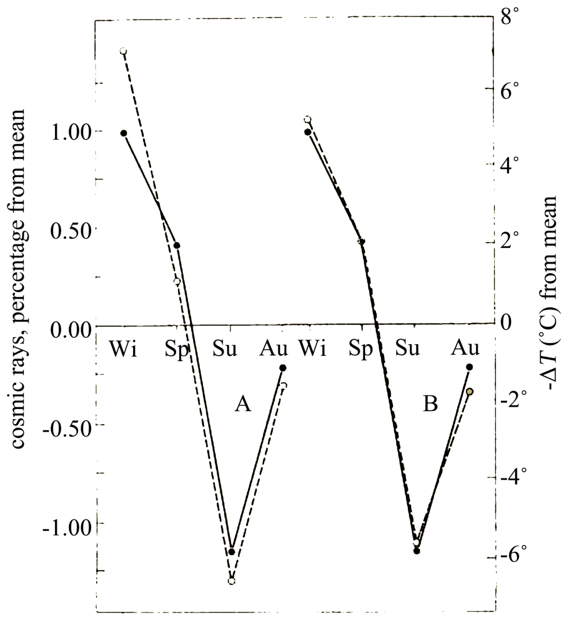

(a)

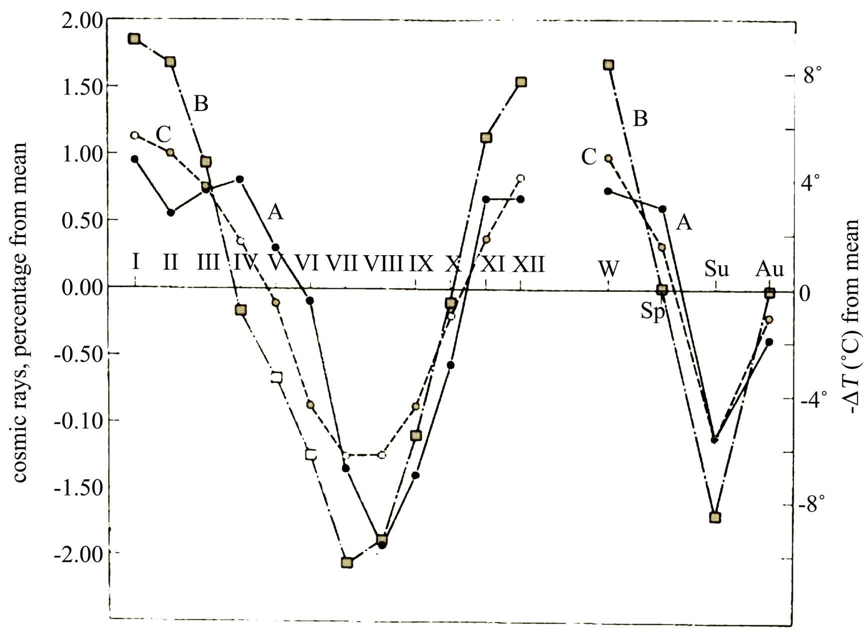

(b)

Figure 3. (a) Seasonal correlation of temperature change of atmosphere and cosmic-ray intensity in partially shielded chambers. A temperature near ground; B mean temperature up to 16 km; (b) Correlation of temperature change at Lindenberg with cosmic intensity at Potsdam. A: CR intensity; B: temperature near ground; C: mean temperature up to 16 km [44].

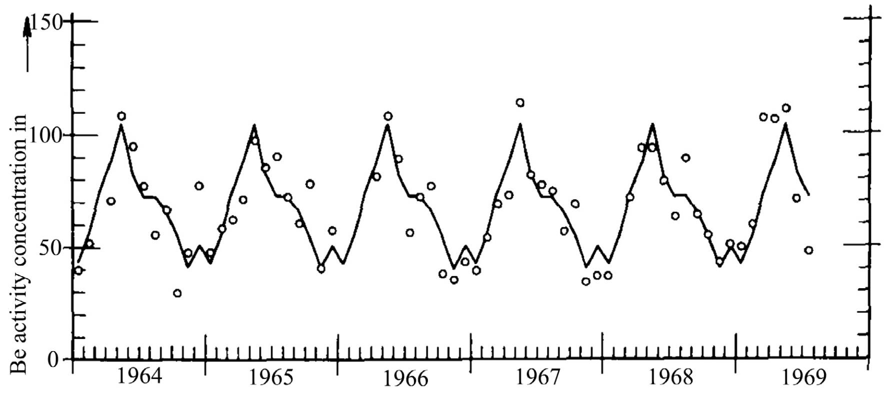

Figure 4. Seasonal fluctuation of the Be activity concentration in the air near the ground. The circles represent the measured values of each month, the solid curve connects the monthly values averaged over almost six years and is therefore repeated periodically [45].

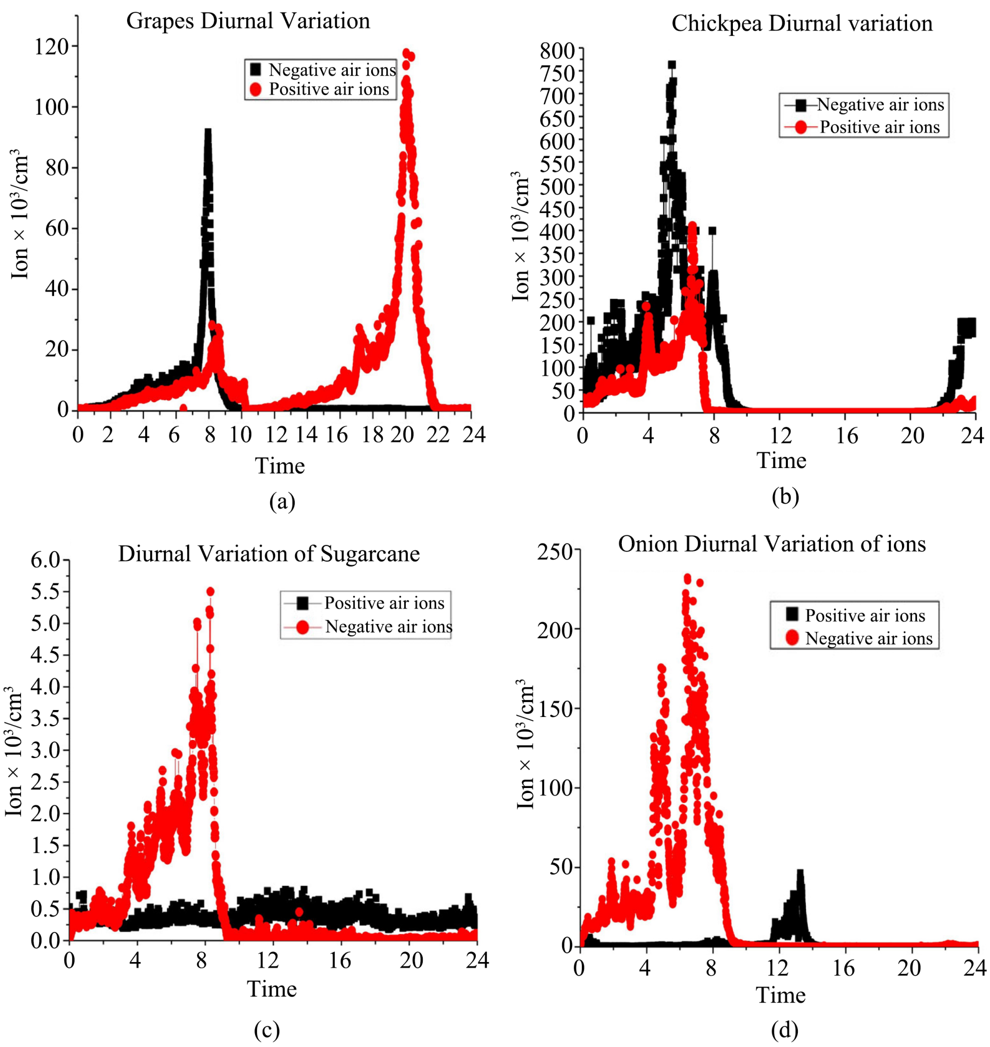

Figure 5. Diurnal variation of measured air ion concentration near definite plants [26]. (a) Diurnal Variation of air ions in Grapes vegetation area; (b) Diurnal variation of air ions in Chickpea vegetation area; (c) Diurnal Variation of air ions in Sugarcane vegetation area; (d) Diurnal variation of air ions in Onion vegetation area.

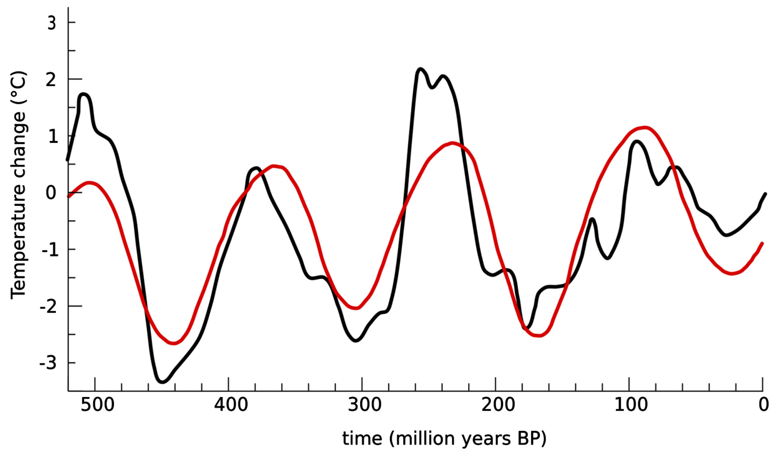

Figure 6. CRs (red) and global temperature (black) assumed from geochemical findings over 5×10^8 years from [24].

Holomorph $L(z, \chi)$, $\xi(z)$ in $z \simeq \lambda$ describe a conductivity plateau as a non-radiative, non-turbulent, non-dissipative potential flow [46]. A conductivity plateau is a plateau of constant temperature where transitions between plateaus cause temperature oscillations. Within the atmosphere global temperature oscillations are proven over 10^8 years as shown in **Figure 6**.

13. Conclusion

As a universe from nothing the zero-energy universe hypothesis proposes that the total amount of energy in the universe is exactly zero. These zero energies are implemented as one-dimensional zero of the Riemann zeta function. Dimensionless unified fields cover all orders of magnitude beyond local experimental setups. Iterated complex quadratic functions as lattices of algebraic units on elliptic curves support a universe as a quantum entangled fractal superfluid. A complex quadratic map written as real curvature $\boldsymbol{R}_{\mu\nu}^4 + 2\mathcal{F}\boldsymbol{R}_{\mu\nu}^2 - \mathcal{G}^2 = 0$ already enters the Friedmann equations. Viewing $\boldsymbol{R}_{\mu\nu} = Rez_k$ as iterated, bifurcated tensile forces yields a matter state with charge and mass locally surrounded by a shower of “CRs” and microwave excitations, in microstructures as well in the universe. An experimental support for a bifurcated spacetime is detected microwaves at QH as well air ionization in vegetation areas. Tensile forces of bifurcated spacetime are felt as CR and CMB. The zero-energy state of the universe described as a nontrivial zero of the Riemann zeta function and related Dirichlet L-functions is reduced to a holomorphic one-dimensional function. This allows to develop the fractal concept of the universe as a zero of $\zeta(z)$ contained in a zero of $\zeta(z)$ iteratively. The resulting Poisson equation allows to define a charge quantum by solving DM by a 2^{2^k} -polar ball with a bifurcation tree of quadrupolar segments 1, 2 → 1’, 2’ of dashed lines as partial magnets. The segments dl_{xy} as a series in the geometric zeta function is the fractal analog of DM for large cloud (monopole) masses due to quadratic mass terms. However, a conductivity plateaus reflects a neutral-like quadrupole-like current as a holomorphic potential. Predicted second sound, CR, CMB at QH have low count rates which solve CCP $\rho_{\exp} \neq \rho_{QS}$ by relating QS to a lap number of k-components. Highly correlated k-components as unstable orbits in the bifurcation tree explain QE by the CCP factor 2^{2^k} for $k = 9$ or $k = 10$. From the mathematical point of view binary substituted Dirichlet L-functions offer a new relation to quantum statistics.

Conflicts of Interest

The author declares no conflicts of interest regarding the publication of this paper.

References

[1] Bhattacharya, J., Bhattacharyya, S. and Minwalla, S. (2011) Dissipative Superfluid Dynamics from Gravity. *Journal of High Energy Physics*, **2011**, Article No. 125. https://doi.org/10.1007/jhep04(2011)125

[2] Ziep, O. (2024) Fractal Zeta Universe and Cosmic-Ray-Charge-Cloud Superfluid. https://www.epubli.com/

[3] Ziep, O. (2025) Matter and Quantum Entanglement. *Journal of Applied Mathematics and Physics*, **13**, 1125-1137. https://doi.org/10.4236/jamp.2025.134059

[4] Einstein, A., Podolsky, B. and Rosen, N. (1935) Can Quantum-Mechanical Description of Physical Reality Be Considered Complete? *Physical Review*, **47**, 777-780. https://doi.org/10.1103/physrev.47.777

[5] Dirac, P.A. (1931) Quantised Singularities in the Electromagnetic Field. *Proceedings of the Royal Society of London. Series A*, *Containing Papers of a Mathematical and Physical Character*, **133**, 60-72.

[6] Weinberg, S. (1989) The Cosmological Constant Problem. *Reviews of Modern Physics*, **61**, 1-23. https://doi.org/10.1103/revmodphys.61.1

[7] Ziep, O. (2024) Nucleosynthesis in Thin Layers. (O. Ziep, Hrsg.) https://www.epubli.com/

[8] Hieb, M. (1995) Feigenbaum's Constant and the Sommerfeld Fine-Structure Constant. https://www.rxiv.org/abs/1704.0365

[9] Manasson, V.A. (2017) An Emergence of a Quantum World in a Self-Organized Vacuum—A Possible Scenario. *Journal of Modern Physics*, **8**, 1330-1381. https://doi.org/10.4236/jmp.2017.88086

[10] Ganter, B. (2020) Deciphering the Fine Structure Constant. epubli. http://inis.iaea.org/search/search.aspx?orig_q

[11] Ganter, B. (2013) The Emergence of the Dimensions and Fundamental Forces in the Universe, an Information-Theoretical Approach for the Explaining of the Quantity Ratios of the Fundamental Interactions, 4. rev. and enl. Ed. http://www.epubli.de/

[12] Martin, J. (2012) Everything You Always Wanted to Know about the Cosmological Constant Problem (but Were Afraid to Ask). *Comptes Rendus. Physique*, **13**, 566-665. https://doi.org/10.1016/j.crhy.2012.04.008

[13] Millikan., R.A. (1913) On the Elementary Electrical Charge and the Avogadro Constant. *Physical Review*, **2**, 109-143. https://doi.org/10.1103/physrev.2.109

[14] Dirac, P.A. (1974) Cosmological Models and the Large Numbers Hypothesis. *Proceedings of the Royal Society A*: *Mathematical*, *Physical and Engineering Sciences*, **338**, 439-446. https://doi.org/10.1098/rspa.1974.0095

[15] Keeper, R. and Ziep, O. (1986) Theory of Quantum Hall Effect. *Physica Status Solidi* (*b*), **133**, 769-773. https://doi.org/10.1002/pssb.2221330239

[16] Moon, M., Li, D., Liao, W., Rigden, A.J. and Friedl, M.A. (2020) Modification of Surface Energy Balance during Springtime: The Relative Importance of Biophysical and Meteorological Changes. *Agricultural and Forest Meteorology*, **284**, Article 107905. https://doi.org/10.1016/j.agrformet.2020.107905

[17] Friedmann, A. (1999) On the Possibility of a World with Constant Negative Curvature of Space. *General Relativity and Gravitation*, **31**, 2001-2008. https://doi.org/10.1023/a:1026755309811

[18] Schönhage, A. (1977) Die Diskriminante einer Matrix. *Archiv der Mathematik*, **28**, 401-408. https://doi.org/10.1007/bf01223943

[19] Ziep, O. (2025) Topological Entropy of Regular Chaotic Quadratic Maps. *Scholars Journal of Physics*, *Mathematics and Statistics*, **12**, 43-58. https://doi.org/10.36347/sjpms.2025.v12i03.002

[20] Einstein, A. (1918) Über Gravitationswellen. Sitzungsberichte der Preussischen Akademie der Wissenschaften zu Berlin, 154.

[21] Ziep, O. (2025) Charge Quanta as Zeros of the Zeta Function in Bifurcated Spacetime. *Journal of Modern Physics*, **16**, 249-262. https://doi.org/10.4236/jmp.2025.162011

[22] Meyer, C. (1970) Bemerkungen zum satz von heegner-stark über die imaginär-quadratischen zahlkörper mit der klassenzahl eins. *Journal für die Reine und Angewandte Mathematik*, **242**, 179-214. https://doi.org/10.1515/crll.1970.242.179

[23] Slavchov, R.I., Dimitrova, I.M. and Ivanov, T.I. (2016) Electrostatics of quadrupolarizable media. arXiv:1610.08650.

[24] Shaviv, N.J. and Veizer, J. (2003) Celestial Driver of Phanerozoic Climate? *GSA Today*, **13**, 4-10. https://doi.org/10.1130/1052-5173(2003)013<0004:cdopc>2.0.co;2

[25] Bisognin, R., Bartolomei, H., Kumar, M., Safi, I., Berroir, J.-M., Bocquillon, E., *et al.* (2019) Microwave Photons Emitted by Fractionally Charged Quasiparticles. *Nature Communications*, **10**, Article No. 1708. https://doi.org/10.1038/s41467-019-09758-x

[26] Patil, G.B., Pawar, S.D., Bhosale, J.L. and Patil, P.G. (2021) Pollution Index and Air Ion Variation in Different Vegetation Area at the Rural Station Bhilawadi (16˚59'N, 74˚28'E). *Journal of Physics*: *Conference Series*, **1964**, Article 032006. https://doi.org/10.1088/1742-6596/1964/3/032006

[27] Ziep, O. (1991) Quantum Transport and Breaking of Space-Time Symmetries. *Mathematical Physics X*: *Proceedings of the Xth Congress on Mathematical Physics*, Leipzig, 6 August 1991, 494.

[28] Ziep, O. (1991) On Fractional Quantization and Triplet Correlations in Quantum Hall Theory. *Physica Status Solidi* (*b*), **168**, K9-K14. https://doi.org/10.1002/pssb.2221680140

[29] Ziep, O. (2023) Linear Map and Spin I. N-Focal Tensor and Partition Function. *Journal of Modern and Applied Physics*, **6**, 1-14. https://www.pulsus.com/scholarly-articles/linear-map-and-spin-i-nfocal-tensor-and-partition-function-11914.html

[30] Riemann, B. (1876) Gesammelte mathematische Werke und wissenschaftlicher Nachlass. BG Teubner.

[31] Hostler, L. (1971) Excited State Reduced Coulomb Green's Function and *f*-Dimensional Coulomb Green's Function in Momentum Space. *Journal of Mathematical Physics*, **12**, 2311-2319. https://doi.org/10.1063/1.1665537

[32] Abrikosov, A.A. (1957) On the Magnetic Properties of Superconductors of the Sec-

ond Group. *Soviet Physics-Journal of Experimental and Theoretical Physics*, **5**, 1174-1182.

[33] Bonch-Bruevich, V.L. (1974) The Benard Problem for Hot Electrons in Semiconductors. *Zhurnal Eksperimental'noi i Teoreticheskoi Fiziki*, **67**, 2204-2214.

[34] Fritzsch, H. (2002) Fundamental Constants at High Energy. In: Papenfuß, D., Lüst, D. and Schleich, W.P., Eds., 100 *Years Werner Heisenberg*: *Works and Impact*, Wiley-VCH Verlag GmbH, 89-95. https://doi.org/10.1002/9783527610853.ch12

[35] Katori, M. (2019) Macdonald Denominators for Affine Root Systems, Orthogonal Theta Functions, and Elliptic Determinantal Point Processes. *Journal of Mathematical Physics*, **60**, Article 013301. https://doi.org/10.1063/1.5037805

[36] Rosengren, H. and Schlosser, M. (2006) Elliptic Determinant Evaluations and the Macdonald Identities for Affine Root Systems. *Compositio Mathematica*, **142**, 937-961. https://doi.org/10.1112/s0010437x0600203x

[37] Laughlin, R.B. (1983) Anomalous Quantum Hall Effect: An Incompressible Quantum Fluid with Fractionally Charged Excitations. *Physical Review Letters*, **50**, 1395-1398. https://doi.org/10.1103/physrevlett.50.1395

[38] Haldane, F.D.M. (2018) A Modular-Invariant Modified Weierstrass Sigma-Function as a Building Block for Lowest-Landau-Level Wavefunctions on the Torus. *Journal of Mathematical Physics*, **59**, Article 071901. https://doi.org/10.1063/1.5042618

[39] Ter Haar, D. (2013) Collected Papers of LD Landau. Elsevier.

[40] Melrose, D.B. (2008) Quantum Plasmadynamics: Unmagnetized Plasmas. Springer. https://doi.org/10.1007/978-0-387-73903-8

[41] Daw, E. (2012) Ultra High Energy Cosmic Rays and The GZK Cutoff. http://www.hep.shef.ac.uk/edaw/PHY206/Site/2012_course_files/phy206rlec5.pdf

[42] https://unsplash.com/

[43] Quanten-Hall-Effekt. https://de.wikipedia.org/wiki/Quanten-Hall-Effekt

[44] Duperier, A. (1941) The Seasonal Variations of Cosmic-Ray Intensity and Temperature of the Atmosphere. *Proceedings of the Royal Society of London*. *Series A*. *Mathematical and Physical Sciences*, **177**, 204-216. https://doi.org/10.1098/rspa.1941.0007

[45] Kolb, V.W. (1970) Jahreszeitliche Schwankungen der ^{7}Be-, ^{54}Mn- und Spaltprodukt-Konzentrationen der bodennahen Luft. *Tellus A*: *Dynamic Meteorology and Oceanography*, **22**, 443-450. https://doi.org/10.3402/tellusa.v22i4.10237

[46] Ziep, O. (2025) Quantized Conductivity as a Neutral Quadrupolar Generator. *Scholars Journal of Physics*, *Mathematics and Statistics*, **12**, 1-5. https://doi.org/10.36347/sjpms.2025.v12i01.001